Optimisation of an electric kick-scooter

Group Number 17

Brake Disc Subsystem: Lidia Dynes Martinez
Frame Subsystem: Sanish Mistry
Wheel Subsystem: Tilly Supple

1 Abstract

In recent years there has been significant growth in the electric transportation industry with electric scooters. The global electric scooter market size is expected to reach USD 28.56 billion by 2025 [1]. From reviews a main drawback is lack of portability of current models compared to traditional scooters and electric skateboards.

As a result of our system optimisation we were able to reduce the mass of the scooter from 12.5 kg to 10.9 kg. This was down to reduction in weight in all 3 sub systems, through dematerialisation and material choices.

2 System-level Problem

The objective is to minimise the mass of the electric scooter. The mass of each subsystem has interior trade-offs, therefore the total mass will consider heat dissipation, structural safety and battery life due to rolling resistance. The total mass will be equal to the mass of the deck (md), the mass of two wheels (md)

$$\begin{aligned}
\textit{min} \quad & f(m_d, m_b, m_w) = m_d(w_d, l_d, l_{bp}, \varrho_d) + \\
& m_b(R_d, R_o, R_i, \theta, t_r) + \\
& 2(m_w(w, d_i, d_0, \varrho_w)) + 6 \\
\textit{s.t.} \quad & g_1(\theta) = -\theta \le 0 \\
& g_2(\theta) = \theta - 72 \le 0 \\
& g_3(R_i) = 0.02 - R_i \le 0 \\
& g_4(R_i, R_o) = R_i - R_o \le 0 \\
& g_5(R_o, R_d) = 0.02 + R_o - R_d \le 0 \\
& g_6(R_d) = (d_i/2) - R_d - 0.02 \le 0 \\
& g_7(t_r) = 0.002 - t_r \le 0 \\
& g_8(t_r) = t_r - 0.004 \le 0 \\
& g_9(E') : 1.33 \times 10^6 - E' \le 0 \\
& g_{10}(d_o) : d_o - 0.25 \le 0 \\
& g_{11}(d_o) : 0.11 - d_o \le 0 \\
& g_{12}(d_i) : d_i - 0.20 \le 0 \\
& g_{13}(d_i) : 0.08 - d_i \le 0 \\
& g_{14}(w) : w - 0.08 \le 0 \\
& g_{15}(w) : 0.04 - w \le 0 \\
& g_{16}(\varrho_w) : \varrho_w - 1500 \le 0 \\
& g_{17}(\varrho_w) : 920 - \varrho_w \le 0 \\
& g_{18}(d_i, d_o) : d_i - d_o \le 0 \\
& g_{19}(w, d_i, d_0, \varrho_w) : \varrho_w \; w((\pi w(\tfrac{d_0}{2})^2 \\
& - \pi(w - 2t)(\tfrac{d_0 - 2t}{2})^2) - ((\pi(2t)(\tfrac{d_i}{2})^2)) \\
& g_{20}(w_d) : w_d - 240 \le 0 \\
& g_{21}(w_d) : 120 - w_d \le 0 \\
& g_{22}(l_{dt}) : l_{dt} - 32 \le 0 \\
& g_{23}(l_{dt}) : 2 - l_{dt} \le 0 \\
& g_{24}(l_{dt}, w) : 40 + w - l_{dt} \le 0 \\
& g_{25}(l_{def}, w_d) : l_{def} - (1\% \, w_d) \le 0 \\
& g_{26}(d_o, d_{bat}, l_{bp}) : 0.5d_o - d_{bat} - l_b - 46 \le 0 \\
& g_{27}(l_{bp}) : 4 - l_{bp} \le 0 \\
& g_{28}(sf_d) : 1 - sf_d \le 0
\end{aligned}$$

2.1 Subsystem Breakdown

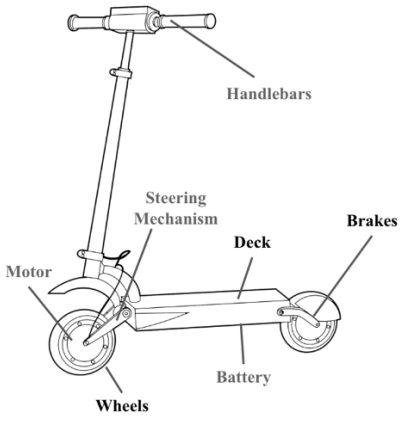

Figure 1 Scooter subsystem

A breakdown of the different components within each subsystem can be found below in Table X:

Table 1 Subsystem Decomposition

Subsystem	Components
Battery	Batteries, Housing, Charging Port
Gearing	Gears, Bearings, Shafts
Frame	Deck, Kickstand, Telescopic Frame, Handlebars
Wheel	Bearings, Tyre, Wheel
Motor	Motor, Housing
Handlebars	Grips, Brake Lever, Accelerator Lever
Brakes	Electric Brake, Rear Friction Brake

2.2 Subsystem Selection

2.2.1 Brake Disc Subsystem

To ensure rider and pedestrian safety on the road the brake system of the scooter should perform properly consistently. The safety of the brakes will be determined by the thermal performance of the disc rotor and the mass of the disk should be minimised to help decrease the overall mass of the scooter.

2.2.2 Deck Subsystem

The main objective of this optimisation study is to minimise the mass of the scooter, this will not only make the scooter more portable, but it will also increase battery life. The scooter deck is the largest and heaviest component within the assembly, therefore the mass of this subsystem should be minimised.

2.2.3 Wheel Subsystem

Another important aspect that contributes to energy consumption is the rolling resistance of the wheels. The wheels were chosen as they contribute significantly to weight to the scooter and the dimensionally constrain the other subsystems.

2.3 Subsystem Interdependencies

Each subsystem is constrained by another. To calculate the mass of the wheels the mass of the frame must be considered and to calculate the mass of the breaks the dimensions of the wheels are required.

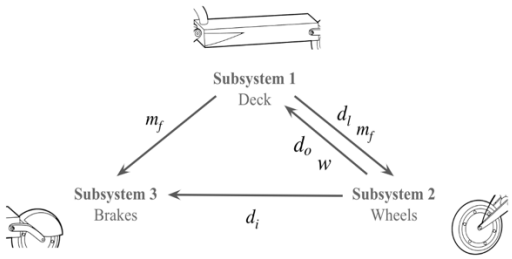

Figure 2.3.1 Subsystem Interdependencies

The width of the wheel is directly linked to the width of the deck and the outer diameter of the wheels influence the ground clearance affecting the battery pack shell thickness.

3 Brake Disk Subsystem

Braking in a scooter takes place due to friction between the brake pad and the rotor disc. This generates heat flux in the disc which causes its temperature and thermal stresses to increase. Sudden braking can cause high temperatures that damage the contact surfaces and decrease the effectiveness of the brakes over time. It is therefore critical to minimise the temperature of the disc to ensure rider safety.

Another important factor when designing an electric scooter, it that the scooter should be as light as possible to improve portability. As such the disk brake should be optimised to be as lightweight as possible to increase user satisfaction.

3.1 Optimisation Formulation

3.1.1 Objective Function

The proposed disc rotor design is based on a solid disk, as shown in Figure 1; several sector-shaped holes will be cut out of the disk to reduce the component's mass.

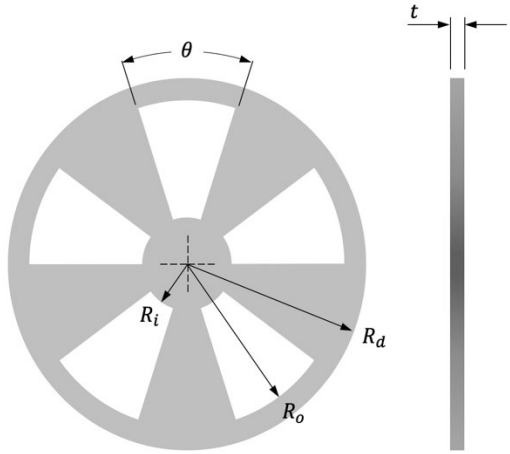

Figure 3.1.1 Schematic of the disc rotor geometry

An optimal brake disc design must strike a balance between a lightweight structure and thermal performance. Increasing the size of the cut-outs will reduce the mass of the component, however, there will be a smaller surface area for the heat to dissipate. To produce a lightweight brake disc, the objective function can be written as:

$$f(R_d, R_o, R_i, \theta, t_r) = [\pi {R_d}^2 - ((\pi\theta/72) \times ({R_o}^2 - {R_i}^2))] \cdot t_r \cdot \varrho_r$$

3.1.2 Design Variables

Variables:

$$R_d, R_o, R_i, \theta, t_r$$

The design constraints of the rotor are divided into three types: geometric, thermal and physical. As the scooter's kinetic energy is transferred to the brake as

thermal energy, the rotor's temperature increases rapidly. The balance between cooling and weight is critical for the disc design. In addition to thermal constraints, the geometry of the rotor should be smaller than the wheel diameter to allow for proper assembly. In total, this model contains five design variables. Optimal disc shape and weight can be found by tuning these variables with the satisfaction of all the constraints mentioned below.

3.1.3 Design Constraints

The design constraints for this study are divided into two types: physical and functional. Physical constraints will ensure the scooter components can fit together during assembly. The chosen constraints are described in Table 1 below:

Table 3.1.3.1 Subsystem physical constraints

g_x	Description
g_1	The cut-out holes should exist
g_2	There should be solid material between the holes
g_3	The inner radius of the hole should be larger than 0.02 m to allow space for attaching the disc to the scooter wheel
g_6	The outer diameter of the disk rotor, R_d, should be less than the inner wheel diameter, d_i to allow for scooter assembly.
g_7	The thickness of the disc should be between the specified values as these are used in industry.

In this subsystem optimisation, di is set to 0.22 m to decouple the two subsystems (brake disc and wheel) and avoid interdependencies. The remaining constraints are all functional and ensure the brake disc can perform under required conditions. The functional constraints are described below in Table 2:

Table 3.1.3.2 Subsystem functional constraints

g_x	Description
g_9	The brake disc should not exceed 250 °C to avoid damaging the brake's contact surfaces
g_{10}	The disc should not deflect more than 5 mm to avoid scratching the wheel hub
g_{11}	The internal stress of the disc should not exceed 50 MPa

The following assumptions were made to simplify the complexity of the model:

- Initial disc temperature is 25 °C
- Heat dissipation from radiation is neglected
- Heat dissipation from convection is constant
- Final speed after braking is 0 km/h
- Braking acceleration is constant

3.1.4 Design Parameters

Parameters: $d_i, \varrho_r, C_r, k_r, w_p$

r, Cr, Cp, kr, kp are determined by the choice of material; *wp* will be assumed when analysing the thermal problems. The complete set of parameter values are written in Table 3 below:

Table 3.1.4.1 Summary of model parameters

Known Parameters	
Initial speed of scooter, v	30 km/h
Braking time, t_b	5 s
Ambient temperature, T_{amb}	25 °C
Thermal conductivity, k	15.5 W/m°C
Density, ϱ_r	7950 kg/m^3
Young's modulus, E_r	197 GPa
Mass of scooter frame, m_f	5 kg
Mass of single wheel, m_w	5 kg
Mass of rider, m_r	100 kg
Calculated Parameters	
Braking force, F_b	2994.8 N
Heat flux, Q	8984.4 J
Area of the brake pad, A_p	$\pi \cdot 0.01^2$ m

3.1.5 Model Summary

$$\textit{min} \quad Mass = f(\mathbf{x}) = [\pi R_d^2 - ((\pi\theta/72) \cdot (R_o^2 - R_i^2))] \cdot t_r \cdot \varrho_r$$

$$\textit{where} \quad \mathbf{x} = (R_d, R_i, R_o, \theta, t_r)$$
$$\mathbf{p} = (Q, t_b, k, T_{amb}, F_b, E, \varrho_r, d_i)$$

$$A = \pi R_d^2 - ((\pi\theta/72) \times (R_o^2 - R_i^2))$$
$$T_{max} = ((Q \cdot t) / (t_b \cdot k \cdot A)) + T_{amb}$$
$$\delta = (F_b \cdot R_d) / (A \cdot E)$$
$$\sigma_{max} = (6 \cdot F_b) / ((\sin(\theta/2)) \cdot t^2)$$

$$\textit{s.t.} \quad g_1(\theta) = -\theta \le 0$$
$$g_2(\theta) = \theta - 72 \le 0$$
$$g_3(R_i) = 0.02 - R_i \le 0$$
$$g_4(R_i, R_o) = R_i - R_o \le 0$$
$$g_5(R_o, R_d) = 0.02 + R_o - R_d \le 0$$
$$g_6(R_d) = (d_i/2) - R_d - 0.02 \le 0$$
$$g_7(t_r) = 0.002 - t_r \le 0$$
$$g_8(t_r) = t_r - 0.004 \le 0$$

$$g_9(\mathbf{x}) = T_{max} - 250 \le 0$$
$$g_{10}(\mathbf{x}) = \delta - 0.005 \le 0$$
$$g_{11}(R_d, \theta, t_r) = \sigma_{max} - 50\ Mpa \le 0$$

3.3 Model Analysis

3.3.2 Monotonicity Analysis

Table 3.3.2.1 Monotonicity table

	R_d	R_i	R_o	θ	t_r
f	+	−	+	−	+
g_1				−	
g_2				+	
g_3		−			
g_4		+	−		
g_5	−		+		
g_6	−				
g_7					−
g_8					+
g_9	U	U	U	U	U
g_{10}	U	U	U	U	U
g_{11}	U			U	U

As seen in the table above, the objective function decreases with respect to Ri and θ and increases with respect to Rd, Ro and tr.

After doing the monotonicity analysis, it is easy to conclude that the minimisation problem is well-constrained. However, by simply looking at the constraints, it is difficult to determine the critical constraints due to g9, g10, and g11; therefore, no variables can be eliminated to reduce the complexity of the model.

3.2 Modelling Approach

3.2.1 Structural Analysis

Where m is the total mass of the scooter including the mass of the driver and v0 is the initial speed of the scooter. Only the back wheel of the scooter has a mechanical brake, therefore, the heat dissipated can be calculated as follows:

Angular velocity of the disc (ω),

$$\omega = u/R_{avg} = 250\ rad/s$$

Total braking force on the disc (Fb),

$$F_b = (KE \cdot 0.5)/d = 2994.8\ N$$

3.2.3 Thermal Analysis

Transient thermal analysis was performed to determine the maximum rise in temperature of the disc after braking. The calculation is shown below. The scooter only has a mechanical brake on its rear wheel, therefore, the scooter only has one brake disk. The total heat flux was also multiplied by 0.5 to get the flux generated by a single pad on the disk brake.

Heat flux generated on each side of the disk (Q),

$$Q = (KE \cdot 0.5)/(t_b \cdot A_p)$$

Where $t = 5\ s$, $A_p = X\ m^2$ and $T_{amb} = 25\ °C$.

3.4 Optimisation Study

MATLAB's fmincon interior-point algorithm was used to optimise this subsystem level problem. The type of problem was taken into account when deciding with algorithm to use. The proposed model is nonlinear constraints and lends itself to gradient-based optimisation methods. Therefore, fmincon was chosen for the optimisation code. To determine if the minimum found was global or simply local to the area, global search was implemented to try to find the global optimum.

3.5 Discussion

The final optimisation result can be found below in Table 3.5.1:

Table 3.5.1 Final optimisation results

R_d	R_o	R_i	θ	t_r	$Mass$
0.04	0.02	0.02	12.56	0.002	0.080

Using the interior-point algorithm within fmincon, Visualising the problem during the optimisation phase became a major challenge during the process. It was difficult to see why the value of each variable changed when initial conditions were altered. Also, different initial values caused the minimum to change. Global search was used to attempt to discover the global minimum of the subsystem however, the minimum mass found was negative although each variable was positive. Due to time constraints, this error was not resolved however, given more time this issue could be addressed.

The analysis could be improved by making the maximum stress assumption more realistic and by developing a metamodel in SolidWorks to determine the points of maximum stress concentration. The assumption that the disk could be modelled as a beam was very rudimental and could be improved to increase the accuracy of the results.

4 Deck Subsystem

4. 1 Optimisation formulation

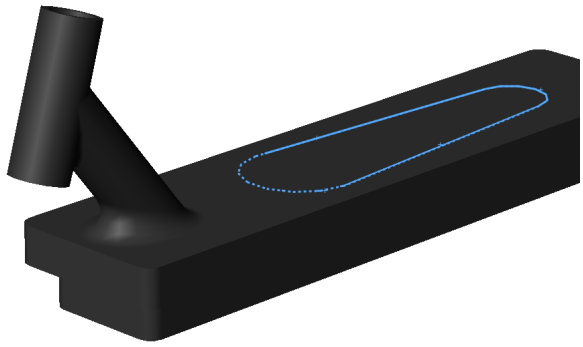

Figure 4.1.1 Diagram of deck

4.1.1 Objective Function

To produce a lightweight design, the objective function is to minimise the mass of the deck. This is in order to improve battery performance and make it easier for users to carry the scooter.

4.1.2 Design Variables

Variables were chosen based on those that could have a large impact on mass including geometric (Deck Width, Deck Thickness, Battery Casing Shell Thickness) and material choice (Density).

4.1.3 Constraints

Constraints were applied to bound the problem was well in addition to the other requirements which were calculated to ensure the electric scooter could be used safely. For example, the Deck Width is be greater than 95th percentile Male Foot Width [15] . The Deck Thickness and the Battery Casing Shell Thickness were bounded by a necessity for a ground clearance below the deck. For safety and preventing structural failure of the deck a deck deflection maximum of 1/300th of the Deck Length [16] and impact force-based stress safety factor were also implemented.

4.1.4 Design Parameters

Parameters were also required to ensure the model optimisation results were realistic and could be comparable to the specification of the Xiaomi Mi Electric Scooter reliably. Deck Length was based on the feet positioning whilst riding of a male user with 95th percentile foot length. The impact force was calculated using a 100kg user (95th percentile male mass [17], this gave 5000N which included a safety factor of 2.0. Battery thickness was based on the thickness of the Mi Scooter battery pack, which is a pack of two layers of AA rechargeable batteries - which have a 15mm diameter [18]. The wheel radius is used in calculating ground clearance, is based on an initial value from the wheel from Subsystem 3.

4.1.5 Model Summary

$$
\begin{aligned}
&min && f(w_d,\ l_{dt},\ l_{bp}, \varrho_d) \\
&where && \mathbf{x} = (w_d,\ l_{dt},\ l_{bp}) \\
& && \mathbf{p} = (l_d, f_i, d_{bat}, \varrho_d, d_o, w) \\
&s.t. && h_1(l_d) : l_d = 600 \\
& && h_2(f_i) : f_i = 3500 \\
& && h_3(d_{bat}) : d_{bat} = 15 \\
& && h_4(\varrho_{d1}) : \varrho_{d1} = 1700 \\
& && h_5(\varrho_{d2}) : \varrho_{d2} = 2700 \\
& && h_6(\varrho_{d3}) : \varrho_{d3} = 2810 \\
& && h_7(\varrho_{d4}) : \varrho_{d4} = 7800 \\
& && g_1(w_d) : w_d - 240 \le 0 \\
& && g_2(w_d) : 120 - w_d \le 0 \\
& && g_3(l_{dt}) : l_{dt} - 32 \le 0 \\
& && g_4(l_{dt}) : 2 - l_{dt} \le 0 \\
& && g_5(w_d, w) : 40 + w - w_d \le 0 \\
& && g_6(l_{def}, w_d) : l_{def} - (1\%\ w_d) \le 0 \\
& && g_7(d_o,\ d_{bat}, l_{bp}) : 0.5d_o - d_{bat} - l_{bp} - 46 \le 0 \\
& && g_8(l_{bp}) : 4 - l_{bp} \le 0 \\
& && g_9(sf_d) : 1 - sf_d \le 0
\end{aligned}
$$

4.2 Modelling approach

4.2.1 Finite Element Analysis

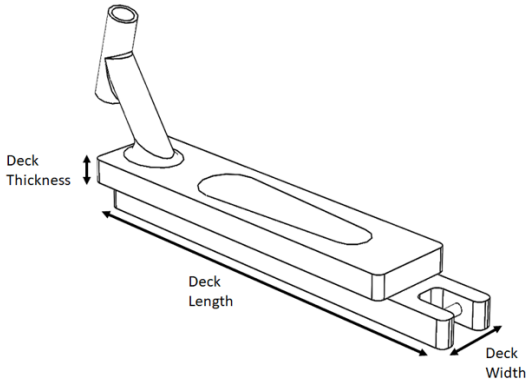

Figure 4.2.1 Diagram of deck

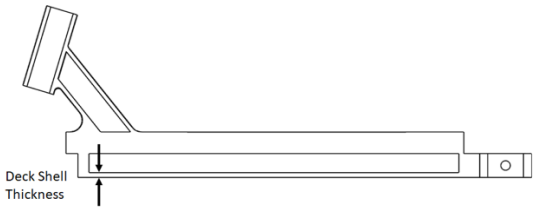

Figure 4.2.2 Cross-section of deck

The deck should be able to withstand a certain impact force without failing at any point in its structure - this is the case if the maximum Von Mises stress in the structure does not exceed the Yield Strength of the chosen material. The structure should also not deflect more than 1% of the structure length. Multiple static simulations will be ran based on different values for the continuous variables within their bounds (Deck Width, Deck Thickness, Battery Casing Shell Thickness); the values which they are run at are calculated using a Latin Hypercube Sampling. These simulations were run by changing the discrete material density variable too. 40 simulations were run, 10 for each material choice.

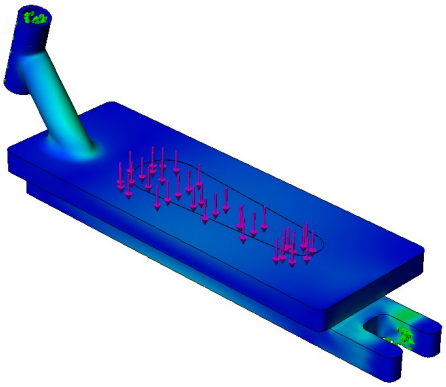

Figure 4.2.3 Static Simulation of Deck

4.2.2 Linear Regression

The data was normalised in order to ensure they were comparable. This was since the values of the different variables where of different magnitudes which would affect the weighting of the various beta values when modelling a regression. Also, the variables used different units which are not directly comparable, normalising the data points allowed for comparison.

Using MATLAB programming, a metamodel was created to confirm the 3 continuous variables have a linear relationship with the mass variable and then linear regression were used to create an equation to link the 3 variables to mass. Additionally, more regression were required to find bounds where the safety factor is greater than 1.0 and the deck deflection is less than 1%. These beta values were then used to create function constraints. This process was completed for the data of all 4 material choices.

Table 4.2.2.1 Normalised Regression Beta Values

Material	**Beta1**	**Beta2**	**Beta3**
Magnesium Alloy	0.382	1.09	0.117
Aluminium Alloy 6061	0.407	1.06	0.288
Aluminium Alloy 7075	0.498	0.952	0.299
Carbon Steel	-0.160	0.496	-0.223

The mvregress function was utilised to ensure the R-squared value was maximised without overfitting the data. The data was also split into train and testing data with a 75:25 split. This further validated the linear models for each material, as they were tested on test data and have high values.

Table 4.2.2.2 Test Data R-Squared Values

Material	**R-Squared Value**
Magnesium Alloy	0.942
Aluminium Alloy 6061	0.985
Aluminium Alloy 7075	0.961
Carbon Steel	0.808

4.3 Problem space exploration

4.3.1 Monotonicity Analysis

Table 4.3.1.1 Monotonicity table

	w_d	l_d	l_{bp}	ϱ_d
f	−	−	−	−
g_1	+			
g_2	−			
g_3		+		
g_4		−		
g_5	−			
g_6	−			
g_7			−	
g_8			+	
g_9	U	U	U	U

From the monotonicity table we can see that all the variables are well bounded since they have a upper and lower bound. With the parameters from the wheel subsystem we can also infer that g5 is

inactive, since it is overridden by g2. There is uncertainty about the nature of the g9 since the simulation results are required to see which variables have positive or negative beta values.

4.4 Optimisation Study

4.4.1 MATLAB programming

Fmincon was used to find the minimum point for each of the materials that meet the requirements of all the constraints. The default, interior points, method was used to produce the result. After removing the normalisation from the data the 4 obtained values for mass were: 3.63 kg for Aluminium Alloy 6061, 4.97 kg for Aluminium Alloy 7075, 12.67 kg for Carbon Steel and 4.52 kg for Magnesium Alloy. Therefore the Aluminium Alloy 6061 value was taken forward.

4.4.2 Validate Final Variable Values

The variable values for these were then remodelled in Solidworks to verify that the functional constraints were all met. The Aluminium Alloy model produced a safety factor of 1.03 which meets the threshold. It also had a 5 times safety factor over the minimum requirement for deflection whilst being within the bounds for the variables.

In order to ensure that minimum point of the function had been chosen a Genetic Algorithm was also run, this also produced the same values for the variables. This shows reliance in the data that was outputted from the Fmincon tool.

Both the Fmincon and Genetic Algorithms worked well to give the same result.

5 Wheel Subsystem

Studies have shown that in electric vehicles, rolling resistance has an influence on energy efficiency [6]. Electric vehicles seek to reduce their rolling resistance to reduce energy loss, giving the user greater energy capacity and therefore greater travel range. The aim of this subsystem optimisation is to reduce the rolling resistance of the wheel whilst reducing the mass.

5.1 Optimisation formulation

5.1 Model Summary Negative Null Form

$$min \qquad f(E',\, d_o,\, d_i, w, \varrho_w \;, t) \;=$$

$$\frac{1}{d_o}(0.9(W_p + W_f + \varrho_w \;\; g((\pi w(\tfrac{d_o}{2})^2 - \pi(w-2t)(\tfrac{d_o-2t}{2})^2) - ((\pi(2t)(\tfrac{d_i}{2})^2))) \;\; \ldots$$

$$\sqrt{\frac{(W_p+W_f+\varrho_w \;\; g((\pi w(\frac{d_o}{2})^2 - \pi(w-2t)(\frac{d_o-2t}{2})^2) - ((\pi(2t)(\frac{d_i}{2})^2))d_o}{wE'}})$$

$$where \quad \mathbf{x} = (d_i\,, d_i\,,\; w,\; E',\; \varrho)$$
$$\mathbf{p} = (W_p, W_f, t)$$

$$s.t. \qquad h_1(W_p):\; W_p = 981$$
$$h_1(W_f,):\; W_f = 17.7$$
$$h_1(t):\; t = 0.015$$

$$g_1(E'):\; E' - 2.18 \times 10^9 \le 0$$
$$g_2(E'):\; 1.33 \times 10^6 - E' \le 0$$
$$g_3(d_o):\; d_o - 0.25 \le 0$$
$$g_4(d_o):\; 0.11 - d_o \le 0$$
$$g_5(d_i):\; d_i - 0.20 \le 0$$
$$g_6(d_i):\; 0.08 - d_i \le 0$$
$$g_7(w):\; w - 0.08 \le 0$$
$$g_8(w):\; 0.04 - w \le 0$$
$$g_9(\varrho_w):\; \varrho_w - 1500 \le 0$$
$$g_{10}(\varrho_w):\; 920 - \varrho_w \le 0$$
$$g_{11}(d_i, d_o):\; d_i - d_o \le 0$$
$$g_{12}(w, d_i, d_0, \varrho_w):\; \varrho_w \; w((\pi w(\tfrac{d_o}{2})^2 - \pi(w-2t)(\tfrac{d_o-2t}{2})^2) - ((\pi(2t)(\tfrac{d_i}{2})^2)) - 0.6 \le 0$$

5.2. Modelling approach

This mathematical model has been derived from first principles.

5.2.1. Problem space exploration

Rolling resistance is a frictional force that opposes the motion of a body moving on wheels. It is the result of the wheel acquiring a flat at its contact with the surface of the road that has symmetrical pressure distribution. As it moves forward the pressure builds up asymmetrically within the wheel

resulting in increasing strain in one side. This results in a resistive force opposing the direction of motion [6].

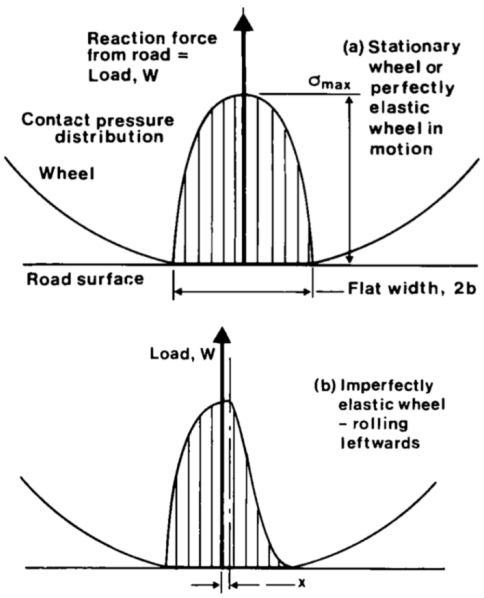

Figure 5.2.1.1 Diagram Showing Flat Contact and Resulting Strain Distribution

This force can be written as a function of the wheel plan area, the material properties of the wheel and the reaction force due to the overall load [7].

$$F = \frac{Wx}{0.5d_o}$$
$$x = 0.6(1 - e^2)b$$
$$b = 0.8\sqrt{\frac{Wd_o}{wE'}}$$
$$therefore: F = \frac{0.6(1-e^2)W\sqrt{\frac{Wd_o}{wE'}}}{d_o}$$

This equation implies that as you increase the width of the wheel (w) you reduce the rolling resistance, however in actuality, because the dimensions are directly related to the load, as they increase, the volume increases, thus the load increases, increasing the rolling resistance. There is therefore an internal balance required. The total load is equal to the load of the person (Wp), the frame (Wf) and the wheel itself (Ww).

$$W_{(total)} = W_p + W_f + W_w$$
$$W_w = mg$$
$$m = \varrho_w V$$

The wheel has been modelled as a shelled cylinder with an internal hole. This closely approximates products on the market [8] where the wheel is surrounds cylindrical hub.

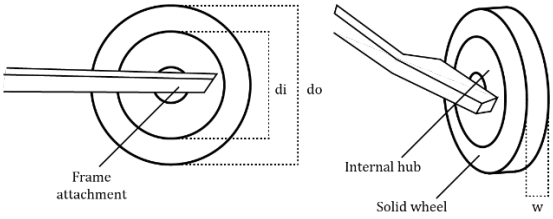

Figure 5.2.1.2 Dimensions of the wheel

The volume of the shelled wheel has been derived from the following diagram where the thickness (t) is taken to be 0.015m, the same as products on the market [9].

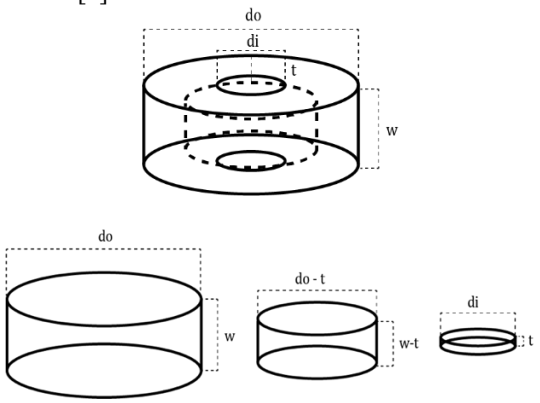

Figure 5.2.1.3 Calculating the Volume of the Wheel

$$V = ((\pi w(\frac{d_o}{2})^2 - \pi(w - 2t)(\frac{d_o-2t}{2})^2) - ((\pi(2t)(\frac{d_i}{2})^2))$$

Therefore, the rolling resistance function can be reformulated to include the mass of the wheel.

$$F = \frac{1}{d_o}(0.9(W_p + W_f + \varrho_w g((\pi w(\frac{d_o}{2})^2 - \pi(w - 2t)(\frac{d_o-2t}{2})^2)$$
$$- ((\pi(2t)(\frac{d_i}{2})^2)))\sqrt{\frac{(W_p+W_f+\varrho_w g((\pi w(\frac{d_o}{2})^2 -\pi(w-2t)(\frac{d_o-2t}{2})^2)-((\pi(2t)(\frac{d_i}{2})^2)))d_o}{wE'}})$$

Density (w) and effective elastic modulus (E') will be selected from the following database of materials. Effective elastic modulus is a function of elastic modulus (E) and Poisson's ratio (v). [7]

Table 5.1.2.1 Diagram Showing Flat Contact and Resulting Strain Distribution [10]

Material	ϱ_w	E	E'
Butyl Rubber	0.92	0.002	2.67E+06
EVA	0.96	0.04	5.27E+07
Isoprene	0.94	0.004	5.33E+06
Natural Rubber	0.93	0.0025	3.33E+06
Neoprene	1.25	0.002	2.67E+06
Polyurethane	1.25	0.003	4.00E+06
Silicone Elastomer	1.50	0.01	1.00E+07

5.2.2. Constraints

Each variable is bounded from both above and below. Dimensional variables are bounded based on their feasible space boundaries and the upper and lower bounds for the material properties are consistent the material database (*Table 2.1*)**.** The functional constraints ensure that the mass will always be a positive number and that the wheel weighs less than current products.

5.2.3. Assumptions

Table 5.2.3.1 Subsystem assumptions

g_3	The maximum height for the wheel must be less than the knee height of a 5th%ile female. [11]
g_4	The minimum outer diameter must be greater than the motor hub plus twice the thickness. [12]
g_5	The internal diameter must be no greater than 0.06m from the hub for attachment.[12]
g_6	The minimum internal diameter must be greater than the motor hub [13].
g_7	The width must be able to fit into the deck slot
g_8	The minimum width must be greater than the thickness of the motor hub.[12]
g_{11}	The inner diameter must be less than the outer.
g_{12}	The mass must be less than 0.6kg. This is the weight of other wheels on the market.[14]
e	The coefficient of restitution is taken to be an average value of 0.5 for calculations.[7]
W_p	The weight of the person has been taken to be the maximum load, 100*g, spread across two wheels
W_f	The weight of the frame is assumed to be 12*g, spread across two wheels.

5.3 Problem Space Exploration

5.3.1 Parametric Analysis

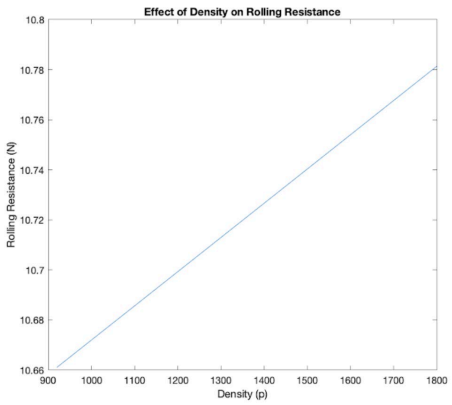

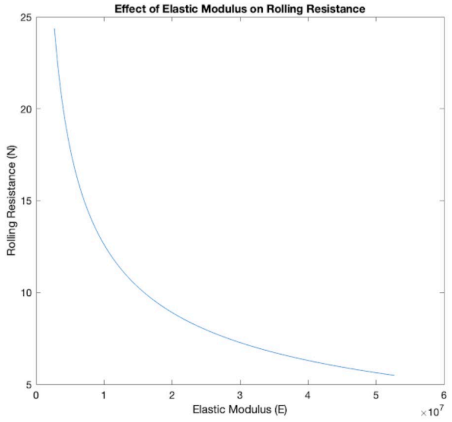

Figure 5.2.3.1 Parametric Analysis of a) Density and b) Elastic Modulus

Keeping all variables constant at their average values a parametric analysis was performed changing the effective elastic modulus and density independently. This showed that, of the two material property variables, the elastic modulus has a significantly greater effect on the rolling resistance of the wheel and density is almost negligible in comparison. Thus, density was made a constant. For calculation purposes this was initially made equal to 1.15 kg/m3, the average of the materials being considered. The correct value would then be inputted corresponding to the optimal Elastic modulus.

5.3.1 Monotonicity Analysis

Table X Monotonicity table

	ϱ_w	E'	d_o	d_i	w
f	+	−	U	U	U
g_1		+			
g_2		−			
g_3			+		
g_4			-		
g_5				+	
g_6				-	
g_7					+
g_8					-
g_{11}			-	+	
g_{12}			+	-	

This monotonicity table showed that g1is active with respect to E' and *g2* is inactive. Therefore, *g1*was made an equality and *g2* was removed.

$$g_1(E'): \; E' = 5.27 \times 10^7$$
$$g_2(E'): \; Inactive$$

This then gave the optimal material to be EVA with a corresponding value of 1.25 kg/m3 for the density.

5.4 Optimisation

5.4.1 Fmincon Interior Point Algorithm

The MATLAB `fmincon` algorithm was used to determine the local minima of the function. This is because it can be simple to implement and fast for solving some constrained optimization problems.

Table 5.4.1.1 Results of Fmincon Interior Points

Variable	Optimal Value
w	0.04
d_o	0.23652
d_i	0.2

Rounded to the nearest *0.01* for ease of manufacture, a width of *0.04m*, an outer diameter of *0.23m* and an inner diameter of *0.2m* delivered a mass of less than 0.6kg and a rolling resistance of *2.1733N*. The run time was found to be 0.097177 seconds.

A problem with `fmincon interior points` is that it can become stuck at a local minimum. It was therefore checked for robustness using `GlobalSearch` to determine the global minimum. It provided the same results with 13 local solver runs converging with a positive local solver at (0.04, 0.2365, 0.2).

5.4.2 Fmincon Sequential Quadratic Programming (sqp) Algorithm

`Fmincon sqp` was then used to test reproducibility and validate the results. It produced the same optimal values but had an improved run time of 0.036354 seconds. This behaved as expected as `sqp` is not a large-scale algorithm.

5.5 Discussion

With the material selection of EVA and updated dimensions of (0.04m, 0.23m.0.2m) found through this optimisation, the rolling resistance compared to the existing product has reduced from *9.3198 N* to *2.1733* N per wheel and the mass has reduced from *1.23kg* to *0.5kg* per wheel. This is an overall reduction in rolling resistance of *76.6%* and a reduction in weight of *58%.*

`Fmincon sqp` was the most computationally inexpensive algorithm that provided that same optimal values and met all conditions.

This optimisation could be improved by altering the geometry of the wheel and adding cut-outs for dematerialisation to further reduce the mass.

6. System Level Optimisation

After the optimisation of each individual section we were able to bring together the values for the variables we had achieved.

Due to the interdependencies in our systems we then used these new values, which were previously set parameters in the subsystem equations.

$$min \quad f(m_d, m_b, m_w) = m_d(w_d, l_d, l_{bp}, \varrho_d) + m_b(R_d, R_o, R_i, \theta, t_r) + 2(m_w(w, d_i, d_0, \varrho_w)) + 6$$

Using *deck mass = 3.7kg* as an input further effects were then seen in the Rolling resistance and size of the wheel.

A final System Mass of 10.9512 kg was found, a substantial reduction on the original 12.5 kg.

Appendix A: Nomenclature

System Level

m_d	Mass of the deck
m_b	Mass of the brake
m_w	Mass of a wheel

Brake Disk Subsystem

R_d	Outer radius of disc (m)
R_o	Outer radius of sector-shaped hole (m)
R_i	Inner radius of sector-shaped hole (m)
θ	Angle of each hole sector (°)
t_r	Disk rotor thickness (m)
ρ_r	Density of rotor (kg/m^3)
h	Heat transfer coefficient (Wm^{-2}K^{-1})
u	Initial scooter speed (km/h)
A_p	Brake pad area (mm^2)
F_{max}	Maximum brake force applied on disc (N)
T_{amb}	Ambient temperature (°C)
T_{max}	Maximum disc brake temperature (°C)
E_r	Young's Modulus of disc rotor (MPa)
t_b	Braking time (s)
d	Braking distance (m)
ω	Disc rotational velocity (rad/s)

Wheel Subsystem

E'	Effective elastic modulus (N/m^2)
E_w	Elastic Modulus (N/m^2)
d_o	Outer Diameter of the wheel (m)
d_i	Inner diameter of the wheel (m)
w	Wheel width (m)
W_f	Weight of the frame (N)
W_p	Weight of the person (N)
W_w	Weight of the wheel (N)
ρ_w	Density of the material (kg/m^3)
V	Volume of the wheel (m^3)
e	Coefficient of restitution
t	Thickness of material (m)

Deck Subsystem

w_d	Deck Width (mm)
l_{dt}	Deck Thickness (mm)
l_{bp}	Battery Pack Thickness (mm)
ρ_d	Density (kg/m^3)
l_d	Deck Length (mm)
f_i	Impact Force (N)
d_{bat}	Battery Diameter (mm)
sf_d	Stress Safety Factor
l_{def}	Deck Deflection (mm)

References

[1] Eve. Electric Scooter Market Worth $28.56 Billion by 2025. October 2018. Available at: https://www.grandviewresearch.com/press-release/global-electric-scooters-marketLast accessed 13/12/18.

[2] Bike Torque Racing. Cast iron or stainless-steel discs? Available from: https://www.biketorqueracing.co.uk/pages/about/btr-tech-station/cast-iron-or-stainless-steel-discs.htm [Accessed 3rd December 2018]

[3] AZO Materials. Stainless Steel - Grade 321 (UNS S32100). Available from: https://www.azom.com/properties.aspx?ArticleID=967 [Accessed 3rd December 2018]

[4] Gear Best. Original Xiaomi M365 Folding Electric Scooter - BLACK. Available from: https://www.gearbest.com/skateboard/pp_596618.html?wid=1433363&currency=GBP&vip=15545041&gclid=CjwKCAjwu5veBRBBEiwAFTqDwZbqdfq9SBN0JZqsq5hAl7JY5vV6_Of1rfHUQcYUfoimZgP0nN_R1xoC4rkQAvD_BwE [Accessed 3rd December 2018]

[5] BikeWalk NC. Rules of the Road from Electric Scooters. Available from: https://www.bikewalknc.org/2018/09/rules-of-the-road-for-electric-scooters/ [Accessed 3rd December 2018]

[6] Rolling Resistance Effect of Tire Road Contact in Electric Vehicle Systems M. Arat, Emmanuel Bolarinwa

[7] Skateboards - a triumph of materials technology N.A. Waterman Fulmer Research Institute

[8] GearBest. 21cm Solid Rear Tire for Xiaomi M365 Electric Scooter. Available: https://uk.gearbest.com/skateboard/pp_1573791.html. Last accessed 13/12/18.

[9] L-faster. Solid Tyre of Xiaomi Scooter. Available:https://www.l-faster.com/items/xiaomi-electric-scooter-mijia-m365-solid-tire/. Last accessed 13/12/18.

[10] Materials Data Book 2003 Edition Cambridge University Engineering Department

[11] Gordon, Claire C. et. al 1988 Anthropometric Survey of U.S. Personnel: Summary Statistics Interim Report. March 1989.

[12] GearBest. Motor / Explosion Proof Wheel Tire Set. Available: https://uk.gearbest.com/skateboard/pp_009133035254.html?wid=1433363&currency=GBP&vip=14752948&gclid=CjwKCAiAo8jgBRAVEiwAJUXKqP34v55At0naUjPVMV73isOOgdyDUUZms624KC07eILjvWxIez8JZxoCZsgQAvD_BwE. Last accessed 13/12/18.

[13] GearBest. / Wheel Hub / Explosion-proof Tire Set. Available: https://uk.gearbest.com/skateboard/pp_009506228148.html?wid=1433363&currency=GBP&vip=14752948&gclid=CjwKCAiAo8jgBRAVEiwAJUXKqOD3PxIJzj7eocKCVD4hANFsZJKnEpBFV_NtjaNZq-mKhbbPkKQudBoCQMwQAvD_BwE. Last accessed 10/12/18.

[14] GearBest. Available: 8.5-inch Solid Electric Scooter Wheel Honeycomb Tire, Available: https://uk.gearbest.com/skateboard/pp_009830248133.html?wid=1433363. Last accessed 10/12/18.

[15] https://www.healthyfeetstore.com/width-sizing-chart.html Last accessed 10/12/18.

[16] https://emedia.rmit.edu.au/dlsweb/Toolbox/buildright/content/bcgbc4010a/04_struct_members/01_beams/page_009.htm Last accessed 10/12/18.

[17] https://www.fsaeonline.com/content/FSAE%20Rules95th_2016.pdf Last accessed 13/12/18.

[18] https://www.all-battery.com/sizechart.aspx, Last accessed 10/12/18.